analytical chemistry

Article

pubs.acs.org/ac

High-Throughput Secretomic Analysis of Single Cells to Assess Functional Cellular Heterogeneity

Yao Lu,[†,⊗] Jonathan J. Chen,[†,⊗] Luye Mu,[†,‡] Qiong Xue,[†] Yu Wu,[†] Pei-Hsun Wu,[§] Jie Li,[∥] Alexander O. Vortmeyer,[∥] Kathryn Miller-Jensen,[†] Denis Wirtz,[§] and Rong Fan*[,†,⊥]

[†]Department of Biomedical Engineering, Yale University, New Haven, Connecticut 06520, United States

[‡]Department of Electrical Engineering, Yale University, New Haven, Connecticut 06520, United States

[§]Department of Chemical and Biomolecular Engineering and the Johns Hopkins Physical Sciences-Oncology Center, Johns Hopkins University, Baltimore, Maryland 21218, United States

[∥]Department of Pathology, Yale School of Medicine, New Haven, Connecticut 06520, United States

[⊥]Yale Comprehensive Cancer Center, New Haven, Connecticut 06520, United States

Supporting Information

ABSTRACT: Secreted proteins dictate a range of cellular functions in human health and disease. Because of the high degree of cellular heterogeneity and, more importantly, polyfunctionality of individual cells, there is an unmet need to simultaneously measure an array of proteins from single cells and to rapidly assay a large number of single cells (more than 1000) in parallel. We describe a simple bioanalytical assay platform consisting of a large array of subnanoliter microchambers integrated with high-density antibody barcode microarrays for highly multiplexed protein detection from over a thousand single cells in parallel. This platform has been tested for both cell lines and complex biological samples such as primary cells from patients. We observed distinct heterogeneity among the single cell secretomic signatures that, for the first time, can be directly correlated to the cells' physical behavior such as migration. Compared to the state-of-the-art protein secretion assay such as ELISpot and emerging microtechnology-enabled assays, our approach offers both high throughput and high multiplicity. It also has a number of clinician-friendly features such as ease of operation, low sample consumption, and standardized data analysis, representing a potentially transformative tool for informative monitoring of cellular function and immunity in patients.

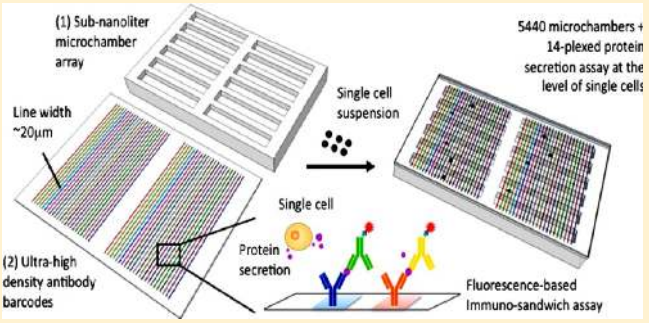

Secreted proteins including cytokines, chemokines, and growth factors represent important functional regulators mediating a range of cellular behavior and cell−cell paracrine/autocrine signaling, e.g., in the immunological system,[1] tumor microenvironment,[2] or stem cell niche.[3] Detection of these proteins is of great value not only in basic cell biology but also for disease diagnosis and therapeutic monitoring. However, because of coproduction of multiple effector proteins from a single cell, referred to as polyfunctionality, it is biologically informative to measure a panel of secreted proteins, or secretomic signature, at the level of single cells. Recent evidence further indicates that a genetically identical cell population can give rise to diverse phenotypic differences.[4] Nongenetic heterogeneity is also emerging as a potential barrier to accurate monitoring of cellular immunity and effective pharmacological therapies,[5,6] suggesting the need for practical tools for single cell analysis of proteomic signatures.

Fluorescence-activated cell sorting (FACS) represents the state-of-the-art for single cell analysis.[7] FACS is typically used to detect and sort cell phenotypes by their surface markers. It has been extended to the detection of intracellular proteins,[7−9] including cytokines within the cytoplasm, by blocking vesicle transport.[10] However, intracellular cytokine staining is not a true secretion analysis, and it also requires cell fixing, which means the cells are no longer alive after flow cytometric analysis and cannot be recovered for further studies. The mainstay of real single cell secretion analysis to date is a simple approach called ELISpot that detects the secretion footprint of individual cells using an immunosandwich-based assay.[11] Immune cells are loaded into a microtiter plate that has been precoated with a layer of primary antibody. After incubation, secreted proteins are captured by the antibodies located proximal to the cells, giving rise to spots indicative of a single cell secretion footprint.[12] Recently, a variant of ELISpot, called FLUORO-Spot, which exploits two fluorescent dyes to visualize protein secretion footprints, enabled a simultaneous dual function

Received: January 9, 2013
Accepted: January 22, 2013
Published: January 22, 2013

   dx.doi.org/10.1021/ac400082e | *Anal. Chem.* 2013, 85, 2548−2556

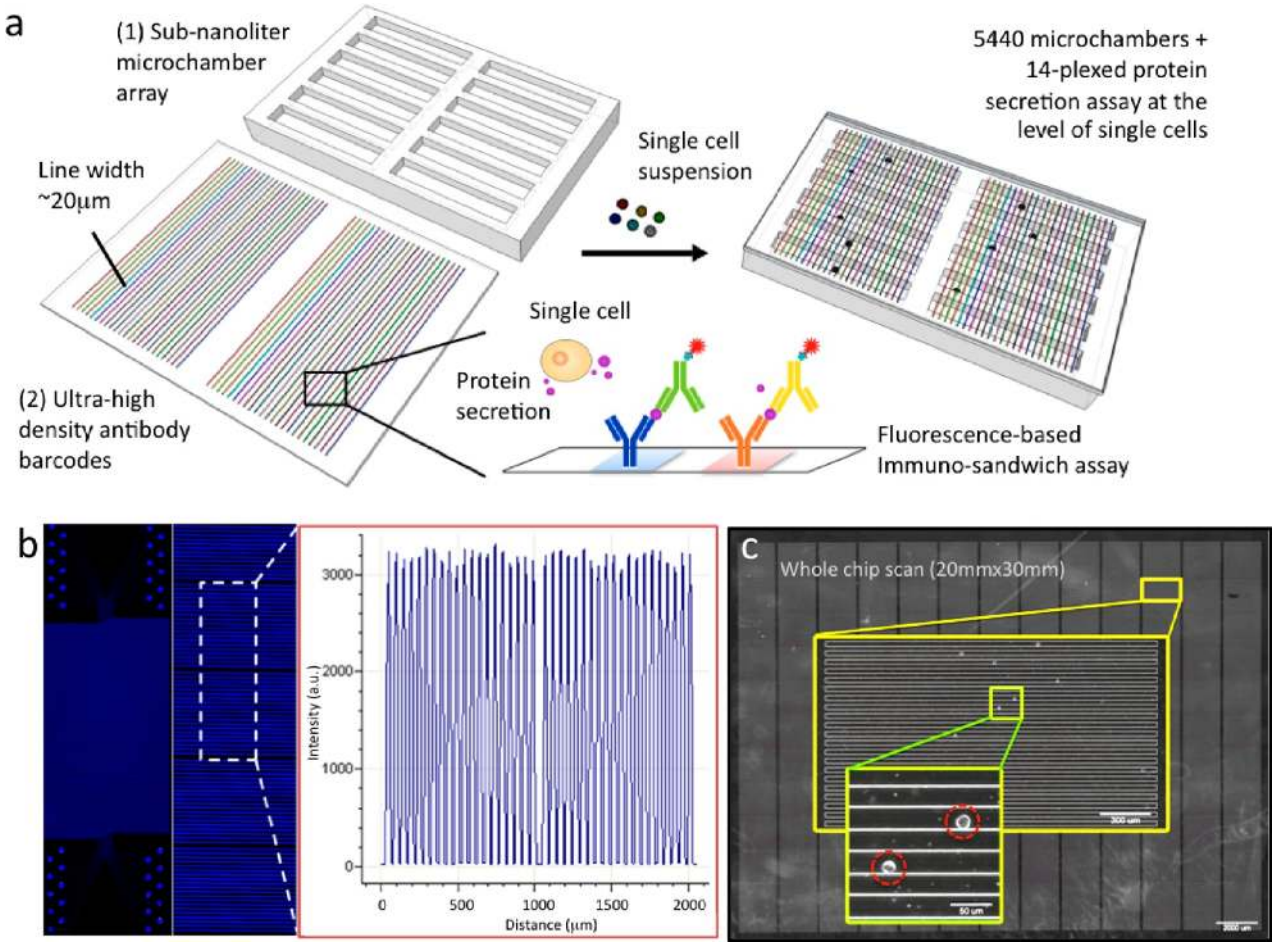

Figure 1. High-throughput multiplexed single cell secretomic assay. (a) Schematic illustration showing integration of a high-density antibody barcode array chip and a subnanoliter microchamber array chip for high-throughput multiplexed protein secretion assay at the single cell level. (b) Scanned fluorescence image showing high uniformity of protein loading across the entire barcode microarray (1 in. × 2 in.). Fluorescently labeled bovine serum albumin (FITC-BSA) was used in this test. (c) Photograph stitched from a large number of individual pictures collected by an automated, motorized phase contrast microscope. Together it covers the entire subnanoliter microchamber chip that was loaded with human immune cells (U973). Scale bar 2 mm. The first enlarged image shows a column of microchamber array (scale bar 300 μm). The second enlarged image shows individual cells loaded in microchambers (scale bar 50 μm).

analysis. Highly multiplexed measurements of proteins secreted from a population of cells can be done using an encoded bead assay such as the Illumina VeraCode system[13] or antibody microarrays manufactured using a pin-spotting technique.[14,15] However, these highly multiplexed technologies cannot perform single cell measurements. Microfabricated chips have emerged as a new category of single cell analytic technologies.[16−21] A prototype microchip has demonstrated the feasibility of the multiplexed protein secretion assay and revealed significant polyfunctional heterogeneity in phenotypically similar immune cells from patients,[22,23] pointing to the urgent need for single cell secretion profiling in clinical diagnosis and therapeutic monitoring. However, these microchips either lack sufficient throughput or multiplicity or require sophisticated operation, precluding widespread application in cell biology and clinical evaluation of cellular functions.

Herein we describe a high-throughput single-cell secretomic analysis platform that integrates a subnanoliter microchamber array and high-density antibody barcodes for simultaneous detection of 14 cytokines from more than a thousand single cells in parallel. The chip can be executed in a simple assay "kit" with no need for sophisticated fluid handling or bulky equipment. We demonstrate the utility of this device for analyzing the secretion of human cell lines and primary cell samples dissociated from the fresh tumor of patients. The results reveal that there is distinct heterogeneity among the single cell secretomic signatures of a population and that the correlations obtained between the various proteins studied are in agreement with their functional classifications. This technology builds upon prior successes in antibody barcode-based protein secretion measurement technique[22] but uses simplified schemes of cell capture,[24] quantification, automated data analysis, and eliminates bulky fluid handling systems, resulting in a truly practical and informative tool that may find immediate use in both laboratory research and clinical cellular diagnosis.

RESULTS AND DISCUSSION

Design, Fabrication, and Assembly of a Single-Cell Secretomic Analysis Chip. Our single-cell secretomic analysis device consists of two separate parts (Figure 1a): a high-density antibody barcode encoded glass substrate for surface-bound immunoassay and a subnanoliter microchamber array for capture of single cells. The antibody barcode array slide comprises 30 repeats of barcodes, each of which contains

dx.doi.org/10.1021/ac400082e | Anal. Chem. 2013, 85, 2548−2556

a

Protein	Function	Protein	Function
EGF	Cell growth, proliferation, differentiation	IL-10	Inhibit synthesis of proinflamatory cytokine
FGF	Angiogenesis	IL-12	Stimulates growth and function of NK and T cells
GMCSF	Granulocyte and monocyte production	IL-13	Proliferation of natural killer cells
HGF	Mitogenesis, cell motility, matrix invasion	MCP-1	Recruits monocytes, memory T cells, and dendritic cells
IFN-γ	Macrophage activation	MIF	Macrophage function
IL-1b	Cell proliferation, differentiation, apoptosis	PDGF	Cell proliferation, cell migration, angiogenesis
IL-2	Growth and function of T cells	RANTES	Chemotaxis
IL-4	Stimulates growth and proliferation of B cells and T cells	TGF-a	Epithelial development, neural cell proliferation
L-5	B cell growth, immunoglobulin secretion	TNF-a	Acute phase reaction
IL-6	Acute phase response	TNF-b	Acute phase reaction
IL-8	Chemotaxis	VEGF	Vasculogenesis, angiogenesis

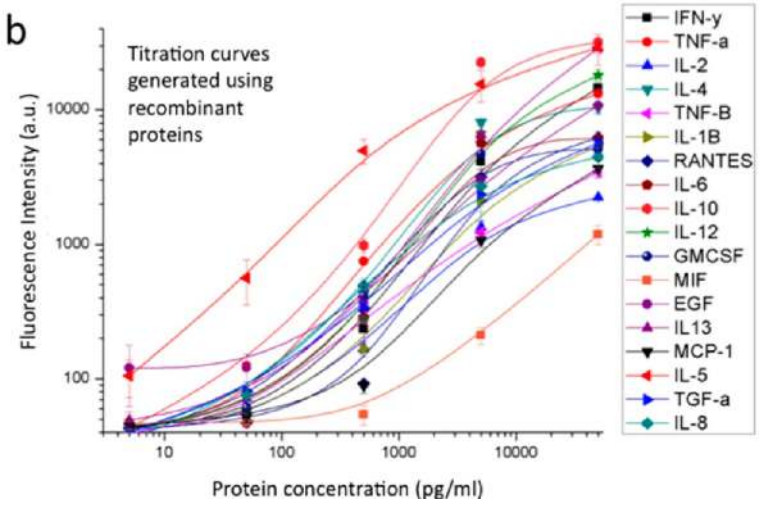

Figure 2. Protein panel. (a) List of all 22 proteins assayed in single cell microchips and their functions in human physiology. (b) Titration curves obtained using recombinant proteins. A total of 18 antibody pairs were validated and 4 others were left out in the titration curves due to the lack of working recombinants. Fluorescence intensity represents the original photon counts averaged from 16 spots for each protein. Error bars indicate 3 × SD.

up to 20 stripes of different antibodies, immobilized on a poly-L-lysine-coated surface. The antibody stripes are 20 μm in width and the pitch size of a full barcode is 1 mm. The microchamber array is a one-layer microchip fabricated by soft lithography[25] from polydimethylsiloxane (PDMS),[25] an optically transparent silicone elastomer widely used for biological microfluidics. It contains 5440 rectangular microchambers, each of which is 1.8 mm, 20 μm, and 15 μm, in length, width, and depth, respectively. These two parts were manufactured independently and combined during the assay such that the barcode slide acts as a disposable test strip and the microchamber array as a reusable device. To use this platform, a drop of single cell suspension (~10^6cells/mL) is directly pipetted onto the surface of the microchamber array chip. The cells fall into the microchambers by gravity, and then the aforementioned antibody barcode array slide is placed antibody-side down on top of the microchambers such that the antibody barcodes are perpendicular to the length of the microchambers. The microchamber is designed to be sufficiently long as to contain at least a full set of barcodes, thereby eliminating the need for precise alignment. Finally this assembly is fixed by two transparent plastic plates with four spring-adjusted screws (Figure S1 in the Supporting Information) and placed in a conventional tissue incubator for single-cell secretion measurement. Proteins secreted from individual cells are captured by the antibody barcodes and read out by incubating with biotinylated detection antibodies and then streptavidin conjugated with a fluorescence probe (e.g., Cy5 in our experiments). As compared to the prototype single cell proteomic chip,[22] this setup does not require a sophisticated microfluidic control system or any bulky equipment to operate and thus is more amenable to widespread use by researchers and clinicians with minimal engineering background.

The high-density antibody barcode array is fabricated using a microchannel-guided flow patterning technique (Supporting Methods in the Supporting Information) modified from the approach reported for patterning DNA barcodes.[26] The flow-patterning chip is a separate PDMS slab that has inlets leading to 20 individual serpentine microchannels in which individual antibody solutions (1 μL each) are precisely metered, added, and flowed through all microchannels in parallel to ensure uniform loading of antibodies on the surface. Fluorescein isothiocyanate labeled bovine serum albumin (FITC-BSA) solution was used to evaluate the patterning quality. The result shows successful fabrication of high-density protein array across a large area (1 in. × 2 in.) and excellent uniformity (<5% in fluorescent intensity) as revealed by the fluorescence intensity line profile (Figure 1b and Figure S2 in the Supporting Information). This ensures the observed protein signal variations (>10%) from the following single cell secretomic assays are attributed to cellular heterogeneity, rather than the nonuniformity of the starting antibody barcode array.

A motorized phase-contrast imaging system has been developed to image all cells in the cell capture chip within 10 min (Figure 1c), and an image analysis algorithm allows for identification of individual cells and their x/y coordinates and

dx.doi.org/10.1021/ac400082e | Anal. Chem. 2013, 85, 2548−2556

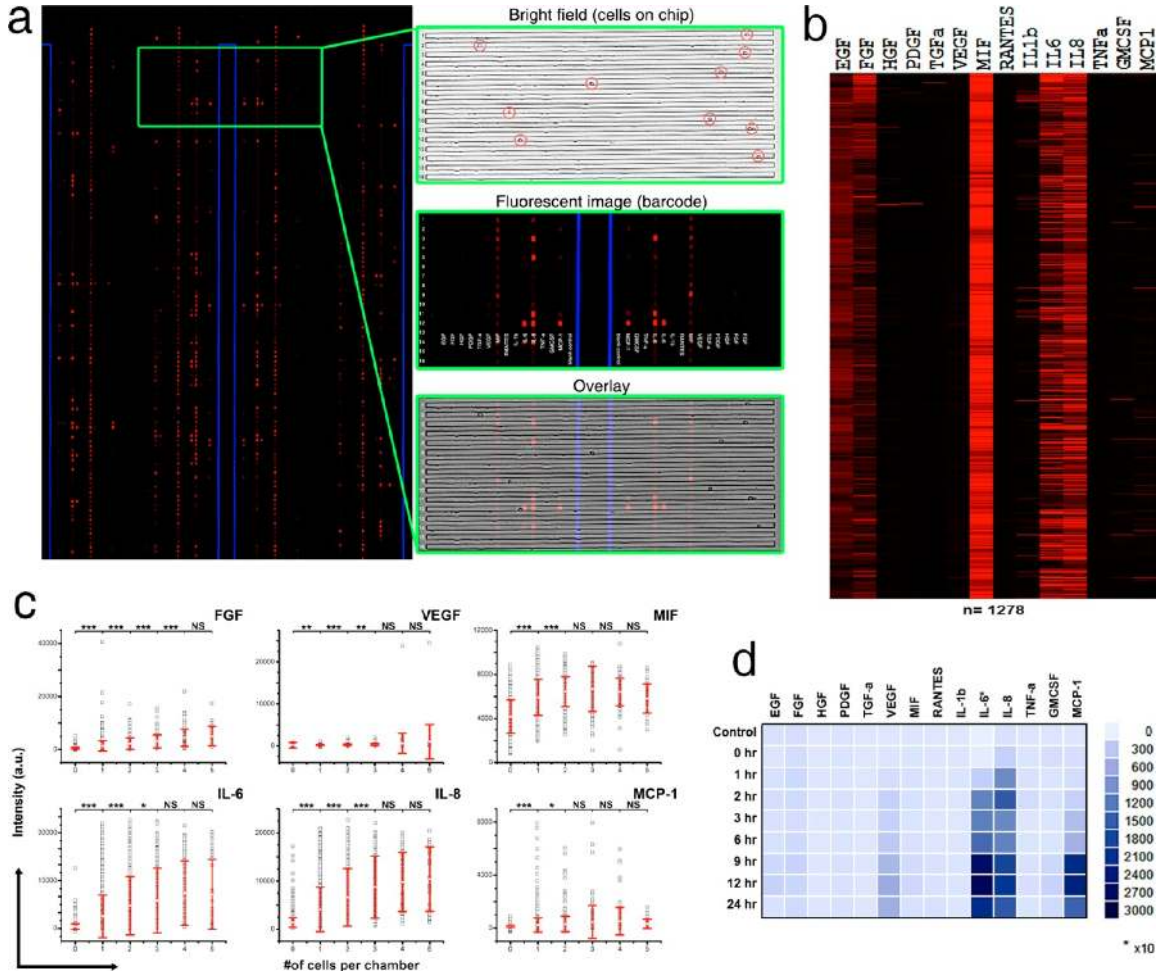

Figure 3. Single-cell secretomic analysis on U87 cell lines. (a) Representative region of the scanned image showing the raw data of single cell secretomic measurement. Three subpanels on the right are optical micrograph, fluorescence image, and overlay for 16 microchambers. (b) Heat map that shows the profile of 14 proteins secreted from 1278 single cells (U87). Each row is a single cell and each column corresponds to a protein of interest. (c) Scatter plots showing fluorescence intensity measured for six selected proteins (FGF, VEGF, MIF, IL-6, IL-8, MCP-1) versus the number of cells in a microchamber. (* $P < 0.05$, ** $P < 0.01$, *** $P < 0.001$) (d) Population kinetics for U87 cell line. Control (MEM medium), secretion supernatant from population at different time points (0 h, 1 h, 2 h, 3 h, 6 h, 9 h, 12 h, 24 h).

counting of cells in each microchamber. The simple microchamber array chip format was chosen because it is easy to operate, but as a consequence it is not possible to ensure that one cell is captured per chamber. However, optimization of cell density in the stock solution readily gives rise to more than 1000 single cell chambers in a microchip (Figure S3 in the Supporting Information), permitting high-throughput analysis of single cells.

Protein Panel and Validation. The proteins assayed by the antibody barcodes are listed in Figure 2a. Assessment of these particular proteins secreted from single cells is of particular importance due to their functions in a range of cellular processes.[27−30] They include cytokines, chemokines, and growth factors involved in a wide range of immunological or pathophysiological processes. Assessment of these proteins secreted from single cells is of importance in the study of cellular immunity and cell−cell signaling networks. In order to simultaneously measure these proteins from single cells, capture antibodies are immobilized on the substrate as a high-density barcode array. Prior to performing single-cell analysis, we validated the assay using recombinant proteins. Individual recombinant protein was spiked into fresh cell culture medium over a 4-log range of concentrations and exposed to the full panel of antibodies in order to assess cross-reactivity, the limit of detection (LOD), and dynamic range. The antibodies with cross-reactivity over 5% (at 5 ng/mL of protein concentration) is eliminated or replaced. Ultimately we obtained a panel of antibody pairs as summarized in Table S1 in the Supporting Information. The titration curves (Figure 2b) demonstrate the feasibility of quantitative measurements of these proteins in the multiplexed array, with a typical measurement range of 3 orders of magnitude. The LOD ranged from 400 pg/mL to below 10 pg/mL depending on the affinity of antibody pairs. On the basis of the volume of a microchamber (~0.54 nL) and the representative detection sensitivity (~10 pg/mL), the amount of protein that can be detected by antibody barcodes in a microchamber is on the order of 5.4 ag, which is approximately equal to ~160 molecules. Thus, our platform has the sensitivity to detect proteins secreted from a single cell (typical copy number $\sim 10^{2-5}$).

Single-Cell Protein Secretomic Analysis on Cell Lines. We first used the single-cell secretomic analysis chip to measure 14 proteins from a human glioblastoma multiforme cell line (U87). In this experiment, up to 10 cells were captured in each microchamber, with 1278 of the microchambers capturing single cells. During the flow patterning of antibody barcodes,

dx.doi.org/10.1021/ac400082e | Anal. Chem. 2013, 85, 2548−2556

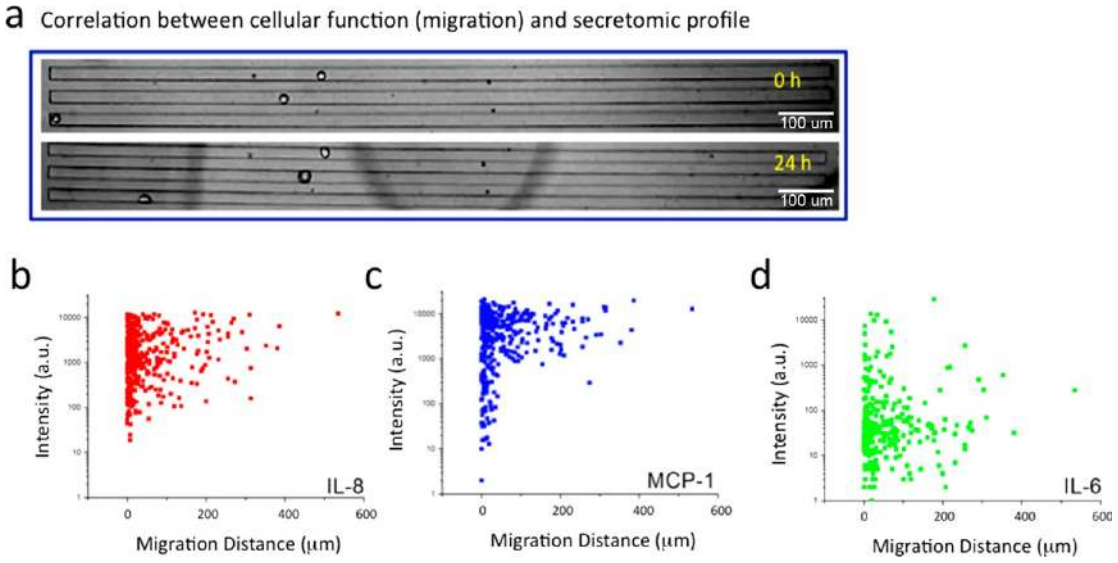

Figure 4. Correlation between protein secretion profiles and cellular migration for A549 cells. (a) Representative optical images showing three single cells (n = 384) before (0 h) and after (24 h) protein secretion assay. (b) Scatter plot showing the fluorescence intensity corresponding to IL-8 secretion versus migration distance of individual cells (P < 0.05). (c) Scatter plot showing a similar analysis on MCP-1 (P = 0.14). (d) Scatter plot showing a similar analysis on IL-6 (P = 0.75). Each dot represents a single cell.

FITC-BSA (0.5 mg/mL) was always flowed in channel 1 to form a continuous line of fluorescence signal serving as both a position reference and an internal quality/uniformity control. As shown in a representative region of the scanned fluorescence image (Figure 3a and Figure S4a in the Supporting Information), both the blue FITC-BSA reference line and the red patterned signals corresponding to protein secretion levels are readily visible. Shown in the same figure are a bright field image of 14 microchambers with cells loaded, the corresponding fluorescent barcode image, and an overlay of the two. The major proteins observed after 24 h of incubation (FGF, VEGF, MIF, IL-6, IL-8, and MCP-1) are mainly pro-inflammatory cytokines or chemoattractant proteins.

We conducted automated quantitation of the fluorescence intensity of each protein in a microchamber using the image analysis software Genepix 6.0. We extracted the secretomic profile for only those microchambers containing single cells and a heat map of the resulting secretion profiles (Figure 3b and Figure S5 in the Supporting Information) indicates the existence of cell−cell variation. While the majority of cells produce IL-6 and IL-8, the level of these proteins varies among individual cells and the secretion of other lower abundance proteins such as MCP-1 and FGF apparently exhibit heterogeneous signatures; only a small fraction of cells express these proteins at high levels. To verify the single cell measurements, a kinetic bulk population secretion measurement was performed in parallel on the supernatant collected from the same cells, incubated over the same time, and measured using a conventional pin-spotted microarray. The result (Figure 3d and Figure S6 in the Supporting Information) also reveals FGF, VEGF, IL-6, IL-8, and MCP-1 as the top five proteins that are all consistent with single-cell analysis although the relative levels are different. However, MIF did not show up in the population assay. Interestingly, we observed that the protein level as measured by fluorescence intensity is not always proportional to the number of cells and sometimes cannot be interpreted by an additive effect (Figure 3c and Figure S7 in the Supporting Information). A secretomic analysis chip was loaded with many more cells, and MIF signal decreases with increasing number of cells in the capture chambers, revealing the possibility of paracrine signaling and the regulation of MIF with an increasing number of cells (Figure S7 in the Supporting Information). This small level of discrepancy is expected as the two assays are not biologically identical (for example, the bulk assay detects the end point protein profile while the single cell assay measures accumulated signals over the period of incubation; the population arrays are subjected to paracrine signaling while single cell measurements are not). Overall, these comparative studies are in good agreement with each other and demonstrated the validity of the single cell secretomic analysis microchip. Another advantage of our platform is that it also measures proteins secreted from multiple cells at the same time. While IL-6 and IL-8 secretion increases with increasing number of cells in a microchamber, the amount of MCP-1 or MIF increase does not change significantly when cell number exceeds 2, suggesting the existence of a possible mechanism similar to "quorum sensing" in which the paracrine mechanism in the multicellular system controls homeostasis.

The single cell secretomic analysis chip was also used to measure two additional cell lines in order to assess the broad applicability of this platform. The first is an immune cell line (U937). The cells are human monocytes, which can be stimulated with phorbol myristate acetate (PMA) to differentiate into functional macrophage cells and then challenged by cytotoxin lipopolysaccharide (LPS) to stimulate cytokine production. This process emulates the inflammatory immune response of human macrophages to Gram-negative bacteria.[31] The major proteins observed are RANTES, TNF-α, MCP-1, IL-6, and IL-8 (Figure S4b in the Supporting Information). While the majority of cells produce RANTES, IL-8, and TNF-α, the level of these proteins varies among individual cells and the secretion of other lower abundance proteins such as MCP-1 and IL-6 exhibit heterogeneous signatures. A bulk population secretion measurement was performed in parallel on the supernatant collected from the same cells to verify the single cell experiments (Figure S8 in the Supporting Information).

dx.doi.org/10.1021/ac400082e | Anal. Chem. 2013, 85, 2548−2556

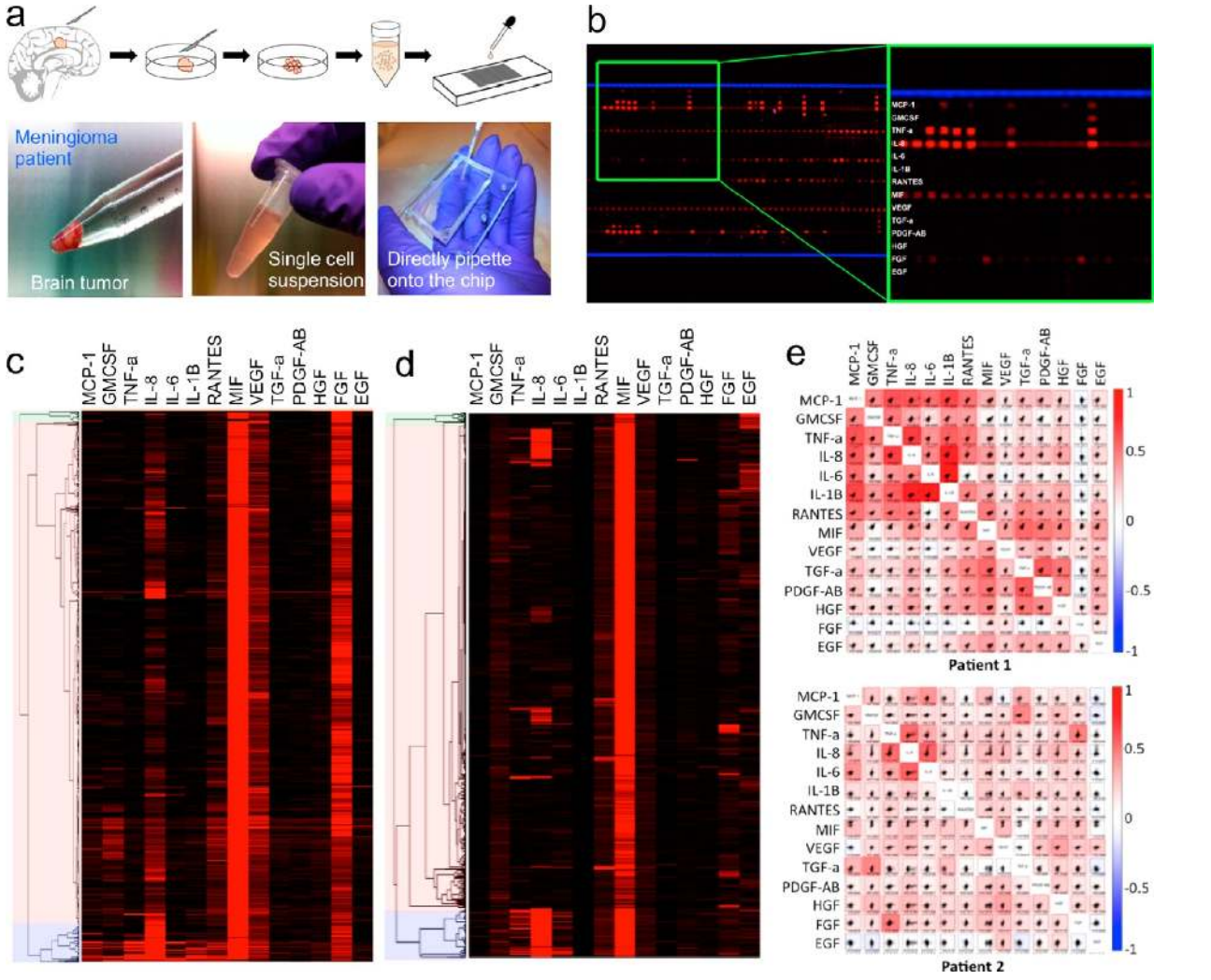

Figure 5. Single-cell secretomic analysis of primary tumor cells from patients. (a) Procedure for processing tissue specimens, preparation of single cell suspension and application of primary cells to the subnanoliter microchamber array chip. (b) Representative region of the scanned image for patient 1. (c and d) Heat maps showing single-cell secretomic signatures of primary tumor cells from two patients (patients 1 and 2), respectively. The data are presented as a result of nonsupervised hierarchical clustering analysis. (e) Histogram plots of individual proteins measured on the sample from Patient 1. (e) Scatter plot matrices showing protein−protein correlation in single cells. Each subpanel is the scatter plot showing the level of a protein versus the other in all single cells measured. The proteins are indicated at the diagonal line. The correlation coefficient is computed as R via a linear regression analysis. The entire matrix is color-coded by red (positive correlation) and blue (negative correlation). The color intensity is proportional to the R value.

The result also reveals RANTES, IL-8, MCP-1, IL-6, and TNF-α as the top five proteins, consistent with the single cell analysis. IL-8 and RANTES secretion increases with an increasing number of cells in a microchamber, and the amount of MCP-1 or TNF-α increases does not change significantly when cell number exceeds 4 (Figure S4c in the Supporting Information). The second is a lung carcinoma cell line (A549) that constitutively produces cytokines or growth factors. Therefore, we measured the basal level secretion from these cells with no stimulation. The major proteins observed are MCP-1, IL-6, IL-8, VEGF, and FGF (Figure S9 in the Supporting Information) that were also validated by the bulk population assay using standard pin-spotted antibody microarray assays (Figure S10 in the Supporting Information). The proteins secreted from A549 cells include both pro-inflammatory cytokines and growth factors, in agreement with the role of lung tumor cells in both maintaining tumor growth and promoting an inflammatory microenvironment. Altogether, the cell line studies demonstrated that our platform is capable of rapid, quantitative, and high throughput analysis of protein secretion profiles in single cells compared to current conventional methods such as ELISpot. Validating our platform with cell lines allow us to expand our sample repertoire to include more complex samples such as tissue specimens from patients.

Correlation between Secretomic Signature and Migratory Property. Although flow cytometry-based single cell analysis allows for multiplexed protein measure, the measured protein profile cannot be directly correlated to the cell's behavior and activity such as migratory property. Our platform utilizes live cell imaging to count captured cells, thus permitting simultaneous measurement of cellular behavior and subsequent correlation to the corresponding protein profile of the same cell. Herein we measure the migration of lung cancer cells (A549) loaded in the single cell secretomic analysis chip by measuring the distance of movement before incubation and after 24 h of incubation (Figure 4a). These cells were seen to

dx.doi.org/10.1021/ac400082e | Anal. Chem. 2013, 85, 2548−2556

adhere to the channel wall and migrate at varying speeds. The results are summarized in a heatmap showing single-cell secretomic profiles sorted by increasing cell migration distance- (Figure S11 in the Supporting Information). We performed *p*-value analysis of cytokine levels in high motility (top 20% over the observed range) vs low motility (bottom 20% of the same range) cells. While the majority of the cells do not migrate, the highly migratory cells are statistically associated with high expression of IL-8 ($P < 0.01$) (Figure 4b). The correlation between the secretion of MCP-1 and cell migration was less significant (Figure 4c,d). IL-6 appears to be negatively associated with cell motility in the scatter plots but does not show statistical correlation using the aforementioned test. These proteins have been linked to the increase of motility and metastatic potential in different cancers,[32−34] and through the investigation of single cell IL-8 secretion, it may be possible to study the secretomic signatures of individual cells linked to metastasis. In brief, our platform for the first time shows simultaneous measurement of protein secretomic signature and phenotypic properties (e.g., migration) of single live cells that can lead to improved understanding of cellular functions and the underlying molecular mechanisms.

Secretomic Profiling of Single Tumor Cells from Clinical Patient Specimens. To expand the utility of our platform to measuring multiplexed secretion in cells derived from complex biospecimens, we also applied our device to the measurement of fresh primary tumor tissue from three patients (Table S2 in the Supporting Information) with a malignant brain tumor, glioblastoma multiforme (patients 1 and 2), or meningioma (patient 3). A portion (<0.2g) of the surgically resected tumor tissue is washed with ice cold phosphate-buffered saline, minced into smaller fractions and then dissociated into a single cell suspension using collagenase (Figure 5a and the Supporting Methods in the Supporting Information). The cells were spun down and resuspended in medium at a density of $\sim 10^6$ cells/mL. Within 1 h of tissue procurement, the single cell suspension is loaded onto the single-cell secretomic analysis device via pipet. After allowing the cells to secrete cytokines for 12 h, the pattern on the barcode array is developed with detection antibodies and scanned. A raw fluorescent image (Figure 5b, patient 1) shows excellent protein signals and similar background compared to the scanned image from cell lines. The antibody barcode array includes 14 proteins as shown in Figure 5b. In this experiment, between 0 and 22 cells were captured within a microchamber, with 1058 of the microchambers capturing single cells. We quantified the fluorescence intensities of each secreted cytokine from each individual channel and then generated a heat map of the single cell secretion profiles (Figure 5c). Unsupervised hierarchical clustering of the single cell secretion profiles resolved three separate populations of cells with varying activity. One cluster of cells (Figure 5c, blue cluster) was generally more active, secreting a wider range of proteins presumably corresponding to a more aggressive phenotype, while the cells indicated by green exhibit the lowest level of cytokine production and may represent more quiescent phenotypes such as tumor stem/progenitor cells.[35] The large fraction indicated by orange are a variety of functional phenotypes. The result from the patient 2 (Figure 5d) shows similarities to the results from patient 1, such as MIF and IL-8 as major proteins but a different pattern in that it has a much reduced production of inflammatory cytokines and a higher level of EGF. The second tier proteins all show distinct cellular heterogeneity. Figures S12 and S13 in the Supporting Information present histograms and scatter plots of individual proteins, which show both the relative levels of proteins and the distributions among the cell population.

We compiled pseudo-three-dimensional scatter plots of the single cell cytokine measurements for the patient primary tumors in the format of flow cytometric plots and formed a 14 × 14 mosaic matrix (Figure 5e). The proteins are shown at the diagonal line, and each panel is a pairwise correlation plot, for each of which we performed a linear regression analysis to yield the *R* value. Then the whole matrix is color-coded by red (positive correlation) and blue (negative correlation), and the color intensity is proportional to *R*. In the patient 1 matrix, all the inflammatory cytokines are apparently associated within one cluster and several growth factors are grouped in a separate cluster, reflecting their functional difference. In the result for patient 2, the pro-inflammatory cytokines, although generally expressed at low levels, also show intercorrelation. Interesting, the secretion of EGF is negatively correlated to pro-inflammatory and chemoattactant proteins (MCP-1, GMCSF, and IL-8). We also analyzed a third sample from a patient (patient 3) with transitional meningioma, which is considered a more homogeneous and less inflammatory tumor. Indeed our results for patient 3 (Figures S14 and S15 in the Supporting Information) show reduced pro-inflammatory cytokine signals. These studies, while still very preliminary, imply the relevance of our results to these cells' physiological functions or pathological condition. Currently surgical treatment remains the most effective therapy of human glioblastoma. Afterward, chemotherapy might be carried out systemically or by putting drug-containing wafers into the surgical cavity to further eradicate invasive tumor cells that have diffused to normal brain tissue.[36] Our platform potentially can distinguish and quantitate invasive cell phenotypes as they generally produce more cytokines as well as different profile of cytokines, which has the clinical value to determine tumor invasiveness and tailor the chemotherapeutic strategy for individual patients. In addition, these proteins that act as the soluble signals to mediate cell−cell communication in tumor microenvironment may be identified as new therapeutic targets for personalized treatment.[37−39]

■ CONCLUSIONS

Single cell proteomic analysis has generally been much more challenging than genetic analysis from single cells, due to the lack of equivalent amplification methods for proteins such as polymerase chain reaction (PCR) for nucleic acids. Recent advance in flow cytometric analysis allows for 34-plexed measurement of protein markers from single cells, but most proteins are either surface receptors or cytoplasmic proteins.[40] Intracellular cytokine staining (ICS) enables indirect assessment of "secreted" proteins, but currently the number of cytokines that can be measured is practically limited to below 10, presumably due to increased nonspecific binding from a large number of antibodies in the limited volume of a single cell. Moreover, unlike protein secretion, it is not a direct measurement of cell function. Thus, multiplexed protein secretion measurement is a missing piece of functional characterization of single cells. It has become increasingly evident that even genetically homogeneous cells can be extremely heterogeneous, leading to many unanswered questions in studying their biology.[41] Studying the secretion profile of single cells can reveal much more about tumor

heterogeneity than studying the signaling patterns of cells in a population wherein the signals become averaged out and all defining information is lost, emphasizing the need for studying single cell secretion.[42,43]

We have described a subnanoliter multiplexed immunoassay chip that enables high throughput, simultaneous detection of a panel of 14 cytokines secreted from over a thousand single cells in parallel. This platform provides significant advantages specific to the detection of secreted proteins and offers information complementary to that obtained through flow cytometry. An example scenario where this device would offer unique advantages is that when a cell separation tool is used to sort out a phenotypically identical cell population using specific surface markers, these cells can then be placed in our device to further reveal cellular heterogeneity at the functional level. For instance, human T cell lineages often display a number of functions, and the complex combinations of multiple functions in a single T cells dictates the "*quality*" of this cell in response to a specific antigen. Recent studies showed that multifunctional T cells often exhibit greater potency and durability.[44] The latest HIV vaccine trials employed the ELISpot technique to count interferon-γ(IFN-γ)-secreting T cells as a means to assess the efficacy of vaccination, but it turns out that most IFN-γ-secreting cells are terminally differentiated effector T cells and have minimal protective effect against viral infection. Our platform represents a promising tool to perform polyfunctional analysis on the cells isolated from a flow cytometer or other separation techniques, e.g., magnetically assisted cell sorting,[45] to bring single-cell protein assay to another level of functional analysis. A potential concern of our platform is that cells are isolated in the sealed microchamber and may experience a condition that affects the normal functioning of primary cells ex vivo. As a bioanalytical tool, our microchip was not intended to perform long-term culture of cells and the typical assay time is a few hours to 1 day. It has been reported that ex vivo assay of primary cells in a sealed and isolated environment do produce proteins over a long time as anticipated for their intrinsic physiological activity,[22,46] and interestingly the cells could gain greater viability in a sealed nanoliter-chamber because it recapitulates the in vivo crowdedness in primary tissue and retains sufficient concentrations of cytokines for more effective autocrine signaling. Thus, our microchip is a promising platform for high-throughput analysis of protein secretion profiles from single primary cells and may assist in differential diagnosis and monitoring of cellular functions in patients.

■ ASSOCIATED CONTENT

Ⓢ Supporting Information

Experimental details for device design, fabrication, and use in single cell secretomic analysis. This material is available free of charge via the Internet at http://pubs.acs.org.

■ AUTHOR INFORMATION

Corresponding Author

*E-mail: rong.fan@yale.edu. Fax: 1-203-431-1061.

Author Contributions

⊗These authors contributed equally to this work.

Notes

The authors declare no competing financial interests.

■ ACKNOWLEDGMENTS

This study was supported by the NIH LINCS Program Technology Center Grant (NIH Grant 1 U01 CA164252; MPI, R.F. and K.M.-J.), the U.S. National Cancer Institute Howard Temin Pathway to Independence Award (NIH Grant 4R00 CA136759; PI, R.F.), a grant from the Bill & Melinda Gates Foundation through the Grand Challenges Explorations Initiative (PI, R.F.), the Alzheimer Association New Investigator Grant, the NIH Grants U54CA143868 (PI, D.W.) and R01 GM084204 (PI, D.W.), and the Single Cell Profiling Core supported by the NIH Grant U54 CA143798 (subaward PI, R.F.). We also acknowledge the Yale Institute for Nanoscience and Quantum Engineering (YINQE) and the Yale Nanofabrication Center to allow us to use their facilities.

■ REFERENCES

(1) Rothenberg, E. V. *Nat. Immunol.* **2007**, *8*, 441.
(2) Hanahan, D.; Weinberg, R. A. *Cell* **2011**, *144*, 646.
(3) Gnecchi, M.; Zhang, Z. P.; Ni, A. G.; Dzau, V. J. *Circ. Res.* **2008**, *103*, 1204.
(4) Niepel, M.; Spencer, S. L.; Sorger, P. K. *Curr. Opin. Chem. Biol.* **2009**, *13*, 556−561.
(5) Gascoigne, K. E.; Taylor, S. S. *Cancer Cell* **2008**, *14*, 111.
(6) Cohen, A. A.; Geva-Zatorsky, N.; Eden, E.; Frenkel-Morgenstern, M.; Issaeva, I.; Sigal, A.; Milo, R.; Cohen-Saidon, C.; Liron, Y.; Kam, Z.; Cohen, L.; Danon, T.; Perzov, N.; Alon, U. *Science* **2008**, *322*, 1511.
(7) Sachs, K.; Perez, O.; Pe'er, D.; Lauffenburger, D. A.; Nolan, G. P. *Science* **2005**, *308*, 523.
(8) Kotecha, N.; Flores, N. J.; Irish, J. M.; Simonds, E. F.; Sakai, D. S.; Archambeault, S.; Diaz-Flores, E.; Coram, M.; Shannon, K. M.; Nolan, G. P.; Loh, M. L. *Cancer Cell* **2008**, *14*, 335.
(9) Irish, J. M.; Hovland, R.; Krutzik, P. O.; Perez, O. D.; Bruserud, Ø.; Gjertsen, B. T.; Nolan, G. P. *Cell* **2004**, *118*, 217.
(10) Prussin, C. *J. Clin. Immunol.* **1997**, *17*, 195.
(11) Sachdeva, N.; Asthana, D. *Front. Biosci.* **2007**, *12*, 4682.
(12) Stratov, I.; DeRose, R.; Purcell, D. F.; Kent, S. J. *Curr. Drug Targets* **2004**, *5*, 71.
(13) Henshall, M.; Gorfain, E. *Genet. Eng. Biotechnol. News* **2007**, *27*, 1.
(14) Chen, S.; LaRoche, T.; Hamelinck, D.; Bergsma, D.; Brenner, D.; Simeone, D.; Brand, R. E.; Haab, B. B. *Nat. Methods* **2007**, *4*, 437.
(15) Liotta, L. A.; Espina, V.; Mehta, A. I.; Calvert, V.; Rosenblatt, K.; Geho, D.; Munson, P. J.; Young, L.; Wulfkuhle, J.; Petricoin, E. F. *Cancer Cell* **2003**, *3*, 317.
(16) Wang, D. J.; Bodovitz, S. *Trends Biotechnol.* **2010**, *28*, 281.
(17) Cheong, R.; Wang, C. J.; Levchenko, A. *Sci. Signal.* **2009**, *2*, pl2.
(18) Love, J. C.; Ronan, J. L.; Grotenbreg, G. M.; van der Veen, A. G.; Ploegh, H. L. *Nat. Biotechnol.* **2006**, *24*, 703.
(19) Lee, S. S.; Horvath, P.; Pelet, S.; Hegemann, B.; Lee, L. P.; Peter, M. *Integr. Biol.* **2012**, *4*, 381.
(20) Rowat, A. C.; Bird, J. C.; Agresti, J. J.; Rando, O. J.; Weitz, D. A. *Proc. Natl. Acad. Sci. U.S.A.* **2009**, *106*, 18149.
(21) Lecault, V.; VanInsberghe, M.; Sekulovic, S.; Knapp, D. J. H. F.; Wohrer, S.; Bowden, W.; Viel, F.; McLaughlin, T.; Jarandehei, A.; Miller, M.; Falconnet, D.; White, A. K.; Kent, D. G.; Copley, M. R.; Taghipour, F.; Eaves, C. J.; Humphries, R. K.; Piret, J. M.; Hansen, C. L. *Nat. Methods* **2011**, *8*, 581.
(22) Ma, C.; Fan, R.; Ahmad, H.; Shi, Q.; Comin-Anduix, B.; Chodon, T.; Koya, R. C.; Liu, C.-C.; Kwong, G. A.; Radu, C. G.; Ribas, A.; Heath, J. R. *Nat. Med.* **2011**, *17*, 738.
(23) Shin, Y. S.; Remacle, F.; Fan, R.; Hwang, K.; Wei, W.; Ahmad, H.; Levine, R. D.; Heath, J. R. *Biophys. J.* **2011**, *100*, 2378.
(24) Balaban, N. Q.; Merrin, J.; Chait, R.; Kowalik, L.; Leibler, S. *Science* **2004**, *305*, 1622.
(25) Unger, M. A.; Chou, H. P.; Thorsen, T.; Scherer, A.; Quake, S. R. *Science* **2000**, *288*, 113.

(26) Fan, R.; Vermesh, O.; Srivastava, A.; Yen, B. K. H.; Qin, L. D.; Ahmad, H.; Kwong, G. A.; Liu, C. C.; Gould, J.; Hood, L.; Heath, J. R. *Nat. Biotechnol.* **2008**, *26*, 1373.
(27) Raman, D.; Baugher, P. J.; Thu, Y. M.; Richmond, A. *Cancer Lett.* **2007**, *256*, 137.
(28) Dranoff, G. *Nat. Rev. Cancer* **2004**, *4*, 11.
(29) Zou, W. *Nat. Rev. Cancer* **2005**, *5*, 263.
(30) Wu, Y.; Lu, Y.; Chen, W.; Fu, J.; Fan, R. *PLoS Comput. Biol.* **2012**, *8*, e1002355.
(31) Aderem, A.; Ulevitch, R. J. *Nature* **2000**, *406*, 782.
(32) Singh, R. K.; Gutman, M.; Radinsky, R.; Bucana, C. D.; Fidler, I. J. *Cancer Res.* **1994**, *54*, 3242.
(33) Li, A.; Dubey, S.; Varney, M. L.; Dave, B. J.; Singh, R. K. *J. Immunol.* **2003**, *170*, 3369.
(34) Waugh, D. J. J.; Wilson, C. *Clin. Cancer Res.* **2008**, *14*, 6735.
(35) Wicha, M. S.; Liu, S. L.; Dontu, G. *Cancer Res.* **2006**, *66*, 1883.
(36) Lesniak, M. S.; Brem, H. *Nat. Rev. Drug Discovery* **2004**, *3*, 499.
(37) Dvorak, H. F. *J. Clin. Oncol.* **2002**, *20*, 4368.
(38) Reardon, D. A.; Wen, P. Y. *Oncologist* **2006**, *11*, 152.
(39) Rich, J. N.; Bigner, D. D. *Nat. Rev. Drug Discovery* **2004**, *3*, 430.
(40) Bendall, S. C.; Simonds, E. F.; Qiu, P.; Amir, E. A. D.; Krutzik, P. O.; Finck, R.; Bruggner, R. V.; Melamed, R.; Trejo, A.; Ornatsky, O. I.; Balderas, R. S.; Plevritis, S. K.; Sachs, K.; Pe'er, D.; Tanner, S. D.; Nolan, G. P. *Science* **2011**, *332*, 687.
(41) Bhatia, S.; Frangioni, J. V.; Hoffman, R. M.; Iafrate, A. J.; Polyak, K. *Nat. Biotechnol.* **2012**, *30*, 604.
(42) Bendall, S. C.; Nolan, G. P. *Nat. Biotechnol.* **2012**, *30*, 639.
(43) Michor, F.; Polyak, K. *Cancer Prev. Res.* **2010**, *3*, 1361.
(44) Seder, R. A.; Darrah, P. A.; Roederer, M. *Nat. Rev. Immunol.* **2008**, 8.
(45) Adams, J. D.; Kim, U.; Soh, H. T. *Proc. Natl. Acad. Sci. U.S.A.* **2008**, *105*, 18165.
(46) Han, Q.; Bagheri, N.; Bradshaw, E. M.; Hafler, D. A.; Lauffenburger, D. A.; Love, J. C. *Proc. Natl. Acad. Sci. U.S.A.* **2012**, *109*, 1607.